THE JOURNAL OF BIOLOGICAL CHEMISTRY
Vol. 280, No. 14, Issue of April 8, pp. 14085–14096, 2005

*Printed in U.S.A.*

# The 14-3-3 Proteins of *Trypanosoma brucei* Function in Motility, Cytokinesis, and Cell Cycle*[S]

Received for publication, November 1, 2004, and in revised form, December 13, 2004
Published, JBC Papers in Press, January 14, 2005, DOI 10.1074/jbc.M412336200

**Masahiro Inoue‡§, Yasuo Nakamura‡¶, Kouichi Yasuda‡¶, Natsumi Yasaka‡‖, Tatsuru Hara‡, Achim Schnaufer**, Kenneth Stuart**, and Toshihide Fukuma‡ ‡‡**

*From the ‡Department of Parasitology, Kurume University School of Medicine, 67 Asahi-machi, Kurume, Fukuoka 830-0011, Japan, ‖Excel Japan Group, Shinjuku, Tokyo, Japan, and **Seattle Biomedical Research Institute, Seattle, Washington 98109-5219*

**The cDNAs for two isoforms (I and II) of the 14-3-3 proteins have been cloned and functionally characterized in *Trypanosoma brucei*. The amino acid sequences of isoforms I and II have 47 and 50% identity to the human τ isoform, respectively, with important conserved features including a potential amphipathic groove for the binding of phosphoserine/phosphothreonine-containing motifs and a nuclear export signal-like domain. Both isoforms are abundantly expressed at approximately equal levels (1–2 × $10^6$ molecules/cell) and localized mainly in the cytoplasm. Knockdown by induction of double-stranded RNA of isoform I and/or II in both bloodstream and procyclic forms resulted first in a reduction of cell motility and then significant reduction in cell growth rates and morphological changes; the changes include aberrant numbers of organelles and abnormal shapes and sizes that mimic phenotypes produced by various cytokinesis inhibitors. Morphological and fluorescence-activated cell sorting analysis of the cell cycle suggested that isoforms I and II might play important roles in nuclear ($G_2$-M transition) and cell (M-$G_1$ transition) division. These findings indicate that the 14-3-3 proteins play important roles in cell motility, cytokinesis, and the cell cycle.**

14-3-3 proteins are a group of dimeric acidic proteins with a relative molecular mass of 30 kDa that bind to phosphoserine/phosphothreonine-containing sequences. 14-3-3 proteins are well conserved and exist in all lower and higher eukaryotes. The proteins are involved in many biological processes acting as molecular chaperones. In mammalian cells, 14-3-3 proteins are crucial for cell survival signaling through binding to proteins such as Raf-1, proapoptotic proteins BAD and BAX, transcription factor FKHR, and cell cycle phosphatase Cdc25 (for a review, see Refs. 1–4). Expression of difopein, a specific inhibitor of 14-3-3/ligand interactions, induces apoptosis in cells, consistent with their important role (5). In plants, 14-3-3 proteins act as important regulators of phosphorylated enzymes of biosynthetic metabolism, ion channels, and regulators of plant growth (6–8). Among yeast, 14-3-3 proteins in *Saccharomyces cerevisiae* are associated with upstream activation of the Ras/mitogen-activated protein kinase signaling pathway (STE 20), a basic helix-loop-helix transcription factor (RTG3), nutrient-regulated transcription factors (MSN2 and MSN4), and cell cycle-dependent filaments in the nucleus (FIN 1) (for a review, see Ref. 9). On the other hand, 14-3-3 proteins in *Schizosaccharomyces pombe* bind to cell cycle-dependent phosphatase (Cdc25) and phospholipase C (9). Moreover, yeast 14-3-3 proteins are functionally interchangeable with the plant and mammalian isoforms (9), suggesting genetic conservation of 14-3-3 molecules in these species.

However, to our knowledge, there have been no functional analyses of protozoan 14-3-3. The protozoan pathogen *T. brucei* is the causal agent of sleeping sickness in humans and Nagana disease in cattle, which hamper African human health and economies, respectively. The disease is spread by the bite of the tsetse fly, in which procyclic forms (PCF)[1] proliferate and differentiate into bloodstream forms (BSF), the life cycle stage that proliferates in the mammalian host. Signal transduction pathways in *Trypanosoma brucei* have not been extensively studied because of low homologies of the sequences to mammalian and yeast sequences, reflecting the ancient divergence of *T. brucei* in the eukaryotic lineage. We have therefore undertaken studies of 14-3-3 in *T. brucei* to identify global signal transduction pathways conserved from humans to trypanosomes as well as divergent pathways that may be novel targets to combat these devastating diseases. To elucidate the functions of 14-3-3 in PCF and BSF cells, we generated and characterized 14-3-3 isoform-specific Tet-inducible double-stranded RNA (dsRNA)-expressing cell clones.

We report here that inhibition of 14-3-3 expression produces cells with an aberrant number of organelles and multinucleated giant cells. Several earlier studies examined the control of nuclear number by protein phosphatases and their association with 14-3-3 molecules. The results of these studies can be summarized as follows: 1) treatment with protein phosphatase inhibitors induced multinucleated cells in *Trypanosoma brucei* and *Trypanosoma cruzi* (10, 11); 2) mammalian 14-3-3s are complexed with protein phosphatase 1 (PP1) and protein phosphatase 2A (12), and 3) PP1 and protein phosphatase 2A play important roles in cell division of mammalian cells and sperm motility (13–15). These findings suggest that protein phospha-

* The costs of publication of this article were defrayed in part by the payment of page charges. This article must therefore be hereby marked "*advertisement*" in accordance with 18 U.S.C. Section 1734 solely to indicate this fact.

*The nucleotide sequence(s) reported in this paper has been submitted to the GenBank™/EBI Data Bank with accession number(s) AB059827 and AB066565.*

[S] The on-line version of this article (available at http://www.jbc.org) contains an additional table and three figures.

§ To whom correspondence may be addressed. Fax: 81-942-31-0344; E-mail: inouedna@med.kurume-u.ac.jp.

¶ These two authors contributed equally to this work.

‡‡ To whom correspondence may be addressed. Fax: 81-942-31-0344.

[1] The abbreviations used are: PCF, procyclic form(s); BSF, bloodstream form(s); dsRNA, double-stranded RNA; dsRNAi, dsRNA interference; PP1, phosphatase 1; FACS, fluorescence-activated cell sorting; Tet, tetracycline; OKA, okadaic acid; GST, glutathione *S*-transferase; PVDF, polyvinylidene difluoride; Ab, antibody.

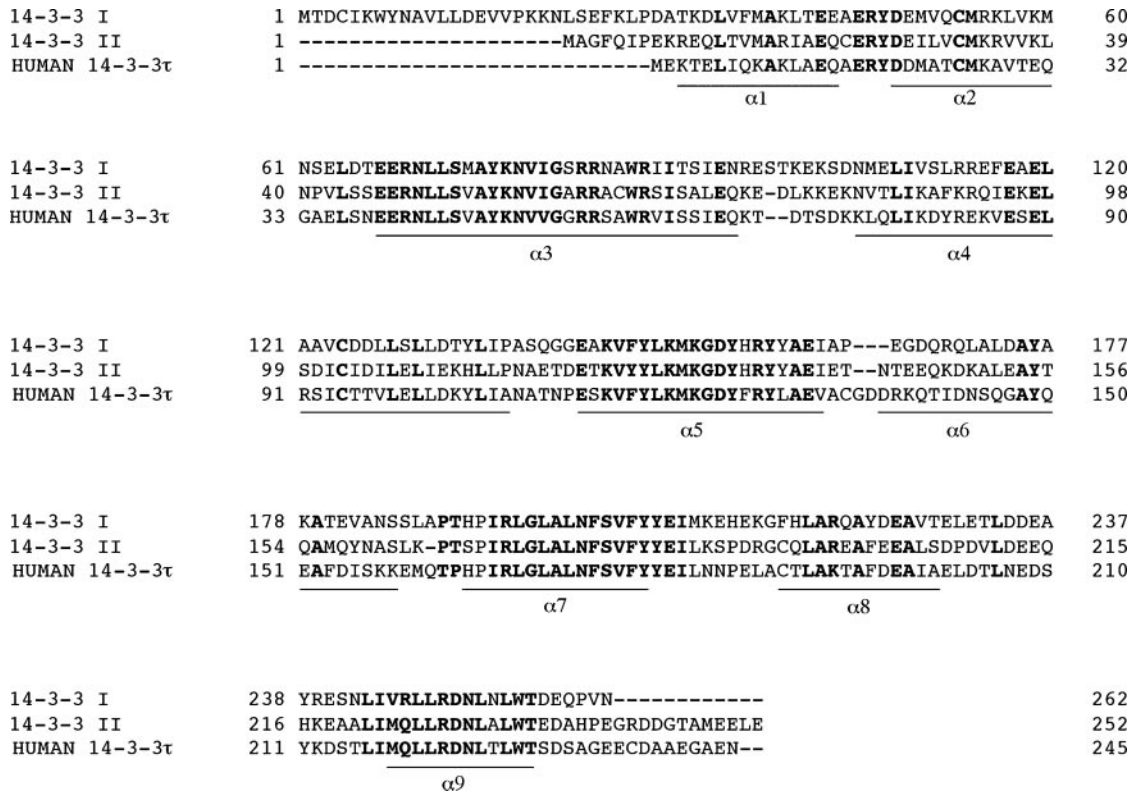


FIG. 1. **Deduced amino acid sequences of 14-3-3 I, II, and human τ.** Each α-helix is *underlined* and *numbered* as described (17, 18). Identical amino acids among the three are shown in *boldface type*. Nucleotide sequences of these clones are deposited in GenBank™ (accession numbers AB059827 and AB066565).

tase might regulate the phosphorylation status of the microtubular network and thereby change protein-protein interaction with microtubule-associated proteins, of which disruption may cause aberrant cytokinesis and cell division.

We also report here that 14-3-3 isoforms I and II play distinctive roles in nuclear division ($G_2$-M transition) and cell division (M-$G_1$ transition), respectively. The cell cycle of trypanosomes has periodic nuclear events, $G_1$, S, $G_2$, and M phases, which are identical to those in the eukaryotic cell cycle (16). However, in contrast to eukaryotes, trypanosomes exhibit a periodic S phase for the kinetoplast, and segregation of the kinetoplast before mitosis is a useful marker of cell cycle progression (16). Cell cycle control in trypanosomes also differs from other eukaryotes, since *T. brucei* cytokinesis is independent of both mitosis and nuclear DNA synthesis (17).

## MATERIALS AND METHODS

### *Cloning of 14-3-3 Genes from T. brucei*

Strain BSF 427 was grown in DDY mice and purified as described previously (18). Approximately $1 \times 10^9$ cells were used to purify total RNA with 20 ml of TRIzol reagent (Invitrogen), and mRNA was purified with the MACS mRNA isolation kit (Miltenyi Biotec Inc., Auburn, CA). One μg of total RNA or 3 μg of mRNA were used to synthesize cDNA using Cap-finder oligonucleotide oligo(dT) (Clontech). The conserved amino acid sequences KMKGDY and VFYYEI of 14-3-3 among yeasts, plants, and mammals were used to design the primers, 5′- AARATGAARGGNGAYTAY-3′ and 5′-DATYTCRTARTARAANAC-3′. PCR was performed under the following conditions: 95 °C for 1 min and then 30 cycles of 95 °C for 15 s, 48 °C for 30 s, and 72 °C for 15 s plus 10 cycles of 95 °C for 15 s, 45 °C for 30 s, and 72 °C for 15 s, followed by 72 °C for 7 min. PCR products were subcloned into pGEM-T Easy (Promega, Madison, WI), and the sequences of 11 clones were analyzed using an ABI 310 sequencer. 5′-Rapid amplification of cDNA end was carried out using *T. brucei* miniexon sequence, 5′-CGCTATTATTAGAACAGTTTCTGTACTATATTTG-3′, and the sequence obtained from the PCR product, 5′-GGTGCCAGTGAACTGTTCGCCA-3′. 3′-Rapid amplification of cDNA end was carried out using the PCR primer of Cap-finder (Clontech) and the sequence obtained from the PCR product, 5′-CACGGAGGTGGCGAACAGTTCA-3′. The 5′- and 3′-rapid amplification of cDNA end products were cloned, and the sequences were examined. The complete coding sequence of 14-3-3 obtained here was then used to screen a genomic library of the PCF 427 strain, which was constructed using λ BlueSTAR BamHI kit (Novagen, Madison, WI). Genomic DNA was completely digested with BamHI, and the above 9-kb fragments were ligated to the λ BlueSTAR. Plaques, which gave rise to five weak and three strong signals in low stringency hybridization conditions, were purified. pBlueSTAR plasmid clones were then obtained from those phage clones by *in vivo* excision. The resultant pBlueSTAR plasmid DNA was digested with several restriction enzymes, including PstI or SalI, to verify the restriction digestion patterns, and Southern blot hybridization was carried out using the coding sequence of 14-3-3. The ~2.7-kb PstI-digested fragment that weakly hybridized and the ~3.0-kb SalI-digested fragment that strongly hybridized with the coding sequence of 14-3-3 obtained by reverse transcription-PCR, were isolated and subcloned in pGEM 3Zf(+) (Promega). Sequences were examined using the EN::TN ⟨KAN-2⟩ insertion kit (Epicenter Technologies). A *T. brucei* cDNA library was constructed using λZipLox, NotI-SalI Arms (Invitrogen). Clones were obtained by hybridizations using two different 14-3-3 coding sequences. The coding sequences of 14-3-3 were also verified with those clones.

### *Construction of GST- and MAL-14-3-3 Expression Vectors*

14-3-3 cDNA, designated as I, II, and human 14-3-3 τ, were amplified with LA Taq (TaKaRa, Kyoto, Japan) using the following primers: I, sense (5′-CGAATTCATGACGGACTGCATCAAGT-3′) and antisense (5′-GGTCTCCACCCTTGTCAGTT-3′); II, sense (5′-CGGAATTCATGGCGGGCTTTCAAATAC-3′) and antisense (5′-GAGCTCACTCCAATTCCTCCATC-3′); τ, sense (5′-GAATTCATGGAGAAGACTGAGCTGATCC-3′ and antisense (5′-CTTAGTTTTCAGCCCCTTCTGCCGCAT-3′). Underlines indicate restriction enzyme recognition sites.

PCR products were subcloned into pGEM-T Easy vector, and sequences were checked. Each EcoRI-digested cDNA fragment was subcloned into pMAL-c2X (New England Biolabs, Beverly, MA), pGEX-1λT (Amersham Biosciences).

### *Antibody (Ab) Production*

Wistar rats were immunized once with 200 μg of GST-I or II fusion proteins. Sera were obtained 3 weeks after immunization and used for this study.

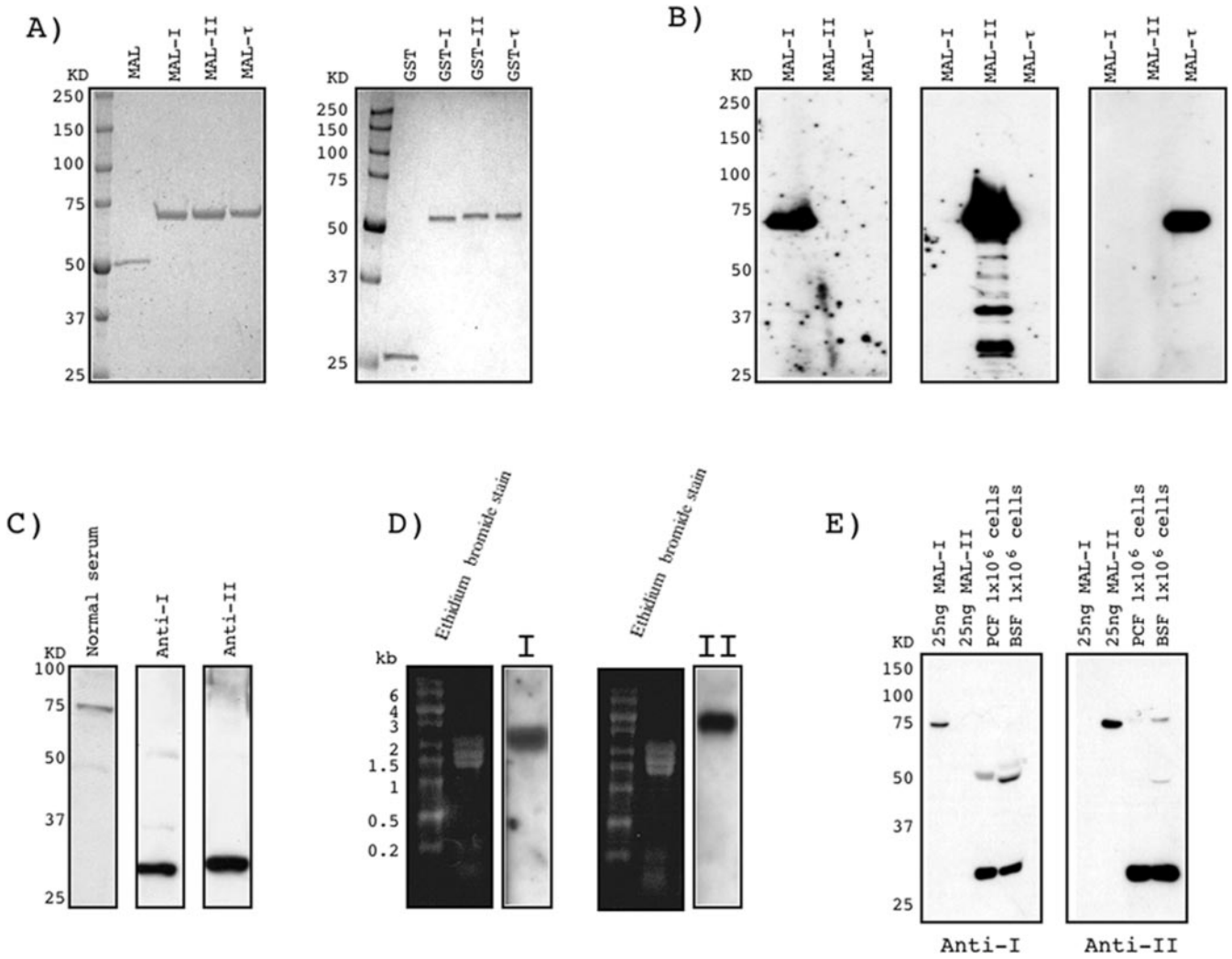


FIG. 2. **Characterization of 14-3-3 proteins.** *A*, Coomassie Blue stain of SDS-PAGE of maltose-binding protein (*MAL*) and GST fusion proteins are as indicated. *B*, Western blot analysis. PVDF membranes were stained with anti-I (*left*), anti-II (middle), and anti-14-3-3 (K-19; Santa Cruz Biotechnology, Inc., Santa Cruz, CA). *C*, Western blot analysis of PCF cell lysates ($5 \times 10^5$ cells). Each PVDF membrane was incubated with antibodies as indicated. *D*, Northern blot analysis of RNA obtained from PCF cells. Five $\mu$g of RNA were applied in each lane. RNA was visualized with ethidium bromide staining. Each blot was hybridized with I or II cDNA as indicated. *E*, semiquantitation of 14-3-3 expressed in PCF and BSF cells. (Western blot data of MAL fusion proteins, PCF, and BSF lysates). The number of cells and amount of each protein are shown as indicated. Each PVDF membrane was incubated with antibodies as indicated.

### *Construction of the pQuadra System*

The overall scheme is shown as a diagram in Supplementary Fig. 1.

*Construction of the pQuadra1 Vector (Contains the Stuffer Fragment)*—As shown in Supplementary Fig. 1, in order to insert a BstXI-BamHI-SrfI/SmaI-BstXI polylinker into a TA-cloning site, the primer pair, 5′-TACCAACTCTATGGATCCGCCCGGGCCAA-3′ and 5′-TACCATCTCTTTGGCCCGGGCGGATCCAT-3′, was annealed and extended using ExTaq polymerase (Takara) and subcloned into pGEM-T Easy vector (Promega) according to the manufacturer's protocol, and the sequence was verified. The resultant plasmid was named pQuadraA. The EM7-blasticidin sequence was generated by PCR from pIB/His A (Invitrogen) using the primer pair 5′-CGTGTTGACAATTAATCATCGGCAT-3′ and 5′-CACGAAGTGCTTAGCCCTCCCACA-3′. The EM7-blasticidin fragment was blunted with T4 DNA polymerase and subcloned into SmaI-digested pQuadraA. The resultant plasmid, pQuadra1, was digested with BstXI, and the released insert fragment was purified from gel for use as a stuffer fragment.

*Construction of pQuadra2 (for Cloning of the Target cDNA)*—In order to insert a second, slightly different BstXI-BamHI-SrfI/SmaI-BstXI polylinker into a TA-cloning site, a second pair of primers, 5′-TACCAATGTGATGGATCCGCCCGGGCCAA-3′ and 5′-TACCATAGAGTTGGCCCGGGCGGATCCAT-3′, was annealed, extended by ExTaq polymerase, and subcloned into pGEM-T Easy, generating pQuadra2. In this report, 14-3-3 I, II, and I + II cDNA fragments were obtained by PCR (plus ligation reaction in the case of I + II) using the following sets of primers: I, sense (5′-GTGGGATCCGGTAATATAACACGAGGCAA-3′ and antisense (5′-GCGGGATCCCTTGGCGTAGGCGTCGAGTGC-3′; II, sense (5′-TAGTGGATCCCAAGCGGTTAAAATGGCG-3′) and antisense (5′-CCTCGGATCCGCGGTCAGGACTCTTCAGGA-3′); I + II, sense (5′-GTGGGATCCGGTAATATAACACGAGGCAA-3′) and antisense (5′-GCTTTCGCGGTTCTCAATAGAAGTG-3′); I + II, sense (5′-CAAAAGAAAAAACAACGGTTAA-3′) and antisense (5′-GGTCGGATCCGCGCTTGAAGGCCTTAATGA-3′).

Those fragments were cut with BamHI and subcloned in pQuadra2 at the BamHI site, and sequences were confirmed. The resultant pQuadra2 vectors containing 14-3-3 fragments were digested with BstXI, and the inserts were purified from the gel.

### *Construction of pQuadra3 Vector (Tet-inducible dsRNAi Vector for T. brucei)*

The luciferase gene in pLew100 (a gift from Drs. Elizabeth Wirtz, Simone Leal, and George Cross (Rockefeller University)) (19) was removed by digestion with BamHI and HindIII followed by blunting and insertion of a *Hin*dIII linker (5′-CAAGCTTC-3′). To remove the internal BstXI sites, the resultant plasmid was digested with BstXI, followed by blunting, and the resultant two fragments were separated and gel-purified. The fragment containing the $\beta$-lactamase gene was treated with shrimp alkaline phosphatase (Amersham Biosciences) and religated with the other fragment. The resultant plasmid was checked by digestion with several restriction enzymes and then digested with HindIII and blunted. A blunted BstXI-BamHI-SrfI-BstXI polylinker was generated by annealing of the primer pair 5′-TACCAGTGTGCTG-

GATCCGCCCGGGCCAT-3′ and 5′-TACCAGTGTGATGGCCCGGGC-GGATCCAG-3′ and extension with ExTaq polymerase followed by T4 DNA polymerase treatment and ligated with the vector. The resultant plasmid was designated pQuadra3. To prepare the vector for the quadric ligation, pQuadra3 was digested completely with BstXI, followed by treatment with shrimp alkaline phosphatase to reduce the background, separated in a 0.6% TAE/agarose gel, and purified from the gel using the QIAEX II gel extraction kit (Qiagen, Hilden, Germany). The inserts generated from pQuadra1 and pQuadra2 were ligated to the digested and purified pQuadra3 vector using the Ligation kit, version 2 (TaKaRa). The ligated fragments were used to transform DH5$\alpha$ competent cells (Toyobo, Japan), and plasmid DNA isolated from the transformants, designated as pQuadra I, pQuadra II, and pQuadra I + II, was analyzed by restriction digestions.

### *Transfection of T. brucei and Analysis of Induced Cultures*

The plasmids pQuadra I, II, and I + II were linearized with NotI and transfected into 29-13 *T. brucei* PCF cells, which express T7 RNA polymerase and Tet repressor, as described (also a gift from Drs. Elizabeth Wirtz, Simone Leal, and George Cross) (19). Sixteen h after transfection, one-quarter of the cells were plated on 96-well plates and selected with 2.5 $\mu$g/ml phleomycin. The same DNA constructs, with the addition of the SV40 enhancer sequence (20) at the EcoRI site, were transfected into 90-13 *T. brucei* BSF cells (also a gift from Drs. Elizabeth Wirtz, Simone Leal, and George Cross) (19). Conditions for transfection of BSF cells were described previously (21).

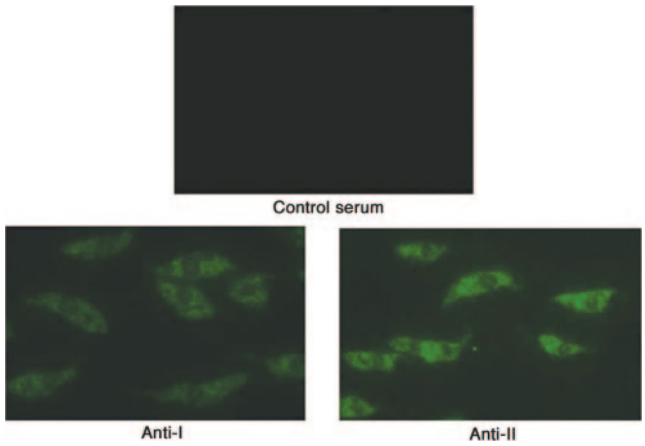


FIG. 3. **Localization of 14-3-3 I (*lower left*) and II (*lower right*) proteins in PCF cells.** Cells were fixed with ice-cold methanol and stained with anti-I, anti-II, or normal rat serum as indicated followed by Alexa 488-labeled secondary Ab (Molecular Probes, Inc., Eugene, OR). Magnification was ×1,000.

### *Fluorescence Microscopy*

The PCF and BSF cells were treated as indicated and placed on 8-well glass slides, dried and fixed with methanol, and stored at −80 °C until use. These slides were then stained with fluorescein isothiocyanate-conjugated anti-$\alpha$-tubulin (clone, DM-1 A) (Sigma) followed by 4′,6′-diamidine-2-phenylindole dihydrochloride. Other slides were stained with anti-I and anti-II rat serum followed by Alexa 488-conjugated anti-rat antibodies (Invitrogen). The stained slides were analyzed by fluorescence microscopy (Olympus BX-60, Olympus, Tokyo) with cooled CCD (Olympus DP-70).

### *Cell Motility Assay*

Cells (0.5 ml) at a concentration of $5 \times 10^6$/ml with Tet induction on day 5 were placed into Acryl cuvettes (19 × 4 × 45 mm) (SARSTEDT), and the cuvettes were incubated at 27 °C for 8 h. The OD in each sample was measured at 600-nm wavelength. The motility index was calculated as follows: OD of Tet+ culture divided by OD of Tet+ culture after mixing the medium.

### *Cell Cycle Analysis of the 14-3-3 Knockdown PCF Cells*

FACS analysis of DNA contents was carried out as follows. Cells were washed twice with phosphate-buffered saline ($Ca^{2+}$, $Mg^{2+}$−), fixed in 30% phosphate-buffered saline, 70% methanol at 4 °C for 1 h, pelleted, and rehydrated. Cells were then treated with 10 $\mu$g/ml RNase at room temperature for 1 h and stained with 10 $\mu$g/ml propidium iodide. The resultant samples were analyzed by FACsort (BD Biosciences) using Cell Quest and ModFIT software (BD Biosciences).

## RESULTS

### *Cloning and Expression of T. brucei 14-3-3*

We cloned two isoforms of 14-3-3 from *T. brucei* 427 cDNA and genomic libraries. They were designated as 14-3-3 I and II,

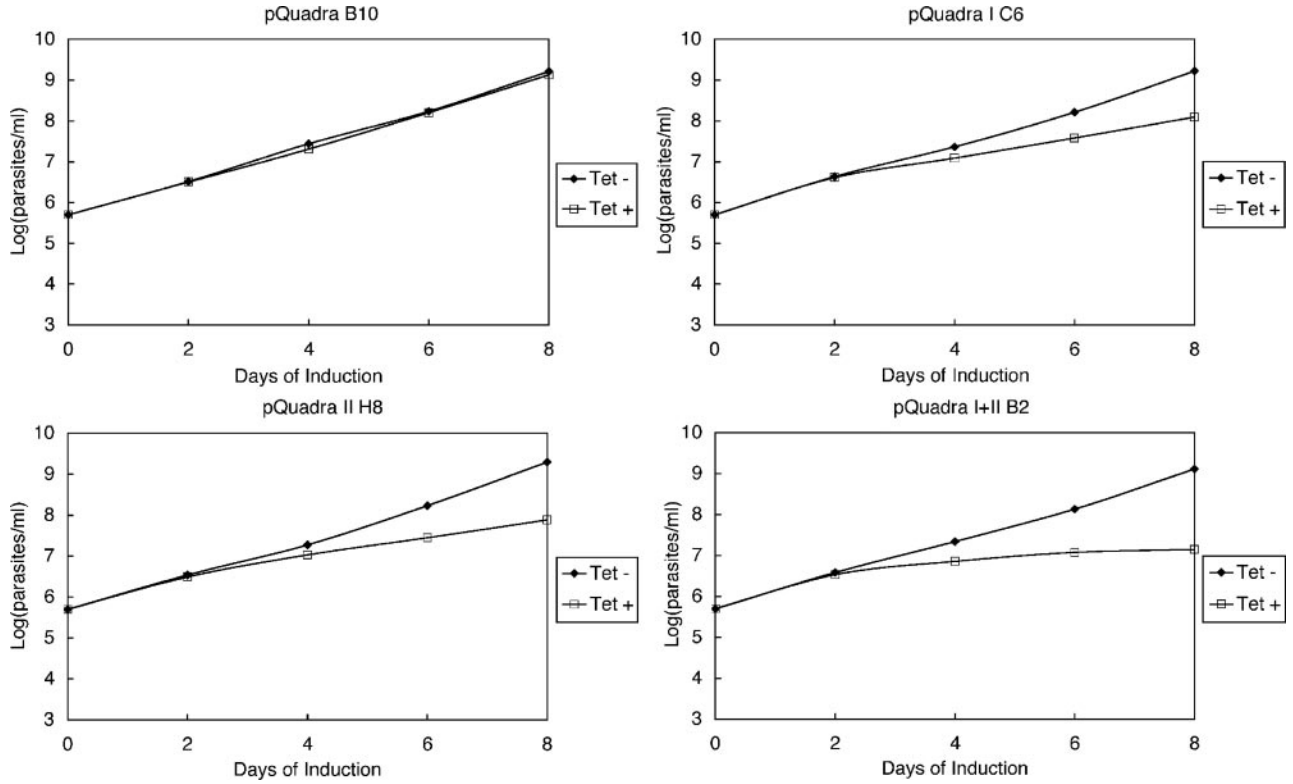


FIG. 4. **Growth curves of representative 29-13 (PCF) cell clones.** Cells were cultured in the presence (1 $\mu$g/ml) or in the absence of Tet. Cells were fed with a 1:10 dilution of fresh medium every 3 days.

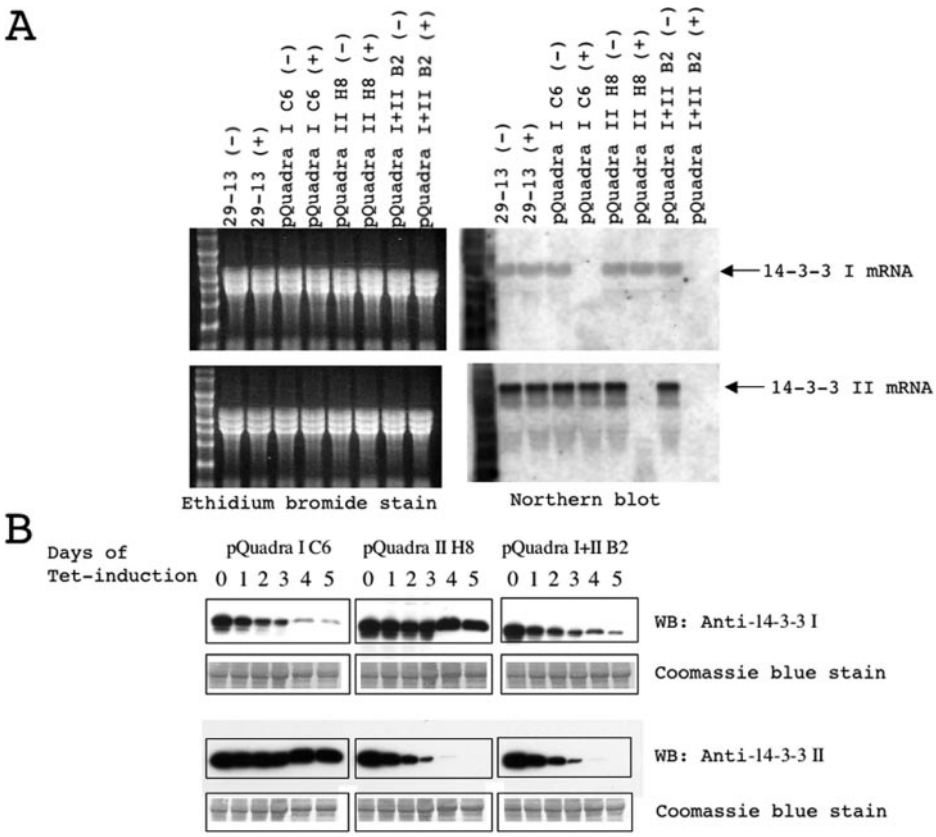


FIG. 5. **Northern and Western blot analysis of 14-3-3 knockdown PCF cells.** *A*, specific reduction of levels of 14-3-3 mRNA of PCF clones after Tet induction on day 1. *Right*, Northern blot of 14-3-3 I (*top*) and II (*bottom*) in each clone. *Left*, ethidium bromide stain of the gel. Five $\mu$g of total RNA were run in each lane. *B*, time course of specific reduction of levels of 14-3-3 proteins after Tet induction. *Top*, Western blot (*WB*) analysis of PCF clones using the indicated Ab on day 0, 1, 2, 3, 4, and 5 of Tet induction. *Bottom*, Coomassie Blue stain of the PVDF membrane. The amount of protein applied in each lane was equivalent to the level of the lysates of $1 \times 10^6$ cells.

respectively (GenBank™ accession numbers AB059827 and AB066565). Genomic library screening with low stringency hybridization conditions and direct sequence analysis of reverse transcription-PCR products using several primers derived from 14-3-3 sequences ensured that only two isoforms existed in *T. brucei* (data not shown). According to sequences available in the Sanger Institute Blast Server (accession numbers TRYPtp25a10ec07.p1k_63), both genes are located on chromosome 11. The start codon was determined from homology with other 14-3-3 sequences isolated from mammals to yeasts, and no potential start codon was found upstream of our determined start codon. Amino acid sequences of I and II have 47 and 50% identity to the human $\tau$ isoform, respectively, and conserved important features of a potential amphipathic groove for the binding of phosphoserine/phosphothreonine-containing motifs, which consists of amino acid residues as follows: $Lys^{77}$, $Arg^{84}$, $Arg^{88}$, $Lys^{150}$, $Asp^{154}$, $Arg^{157}$, $Tyr^{158}$, $Leu^{199}$, $Val^{203}$, $Leu^{244}$, $Leu^{248}$, and $Trp^{256}$ in I and $Lys^{56}$, $Arg^{63}$, $Arg^{67}$, $Lys^{128}$, $Asp^{132}$, $Arg^{135}$, $Tyr^{136}$, $Leu^{174}$, $Val^{178}$, $Leu^{221}$, $Leu^{225}$, and $Trp^{233}$ in II (Fig. 1) (1, 22, 23). Nuclear export signal-like sequences (24) are also conserved and exist in the $\alpha$-helix 9 (Fig. 1). Although the critical amino acid residues required for dimerization are not well conserved, *T. brucei* 14-3-3 proteins dimerize.[2] These data are consistent with evolutionarily conserved features of 14-3-3 proteins: 1) they mainly exist as dimeric forms, 2) they bind to phosphoserine-containing motifs in a sequence-dependent manner, and 3) they contain a nuclear exporting signal (1–4). Thus, they may act as adaptor molecules, increasing or decreasing protein-protein interactions and regulating the subcellular localization of the target proteins and activated or inhibited enzymes, possibly through their binding to phosphoserine/threonine-containing sequence motifs in diverse partners. In order to determine the expression of

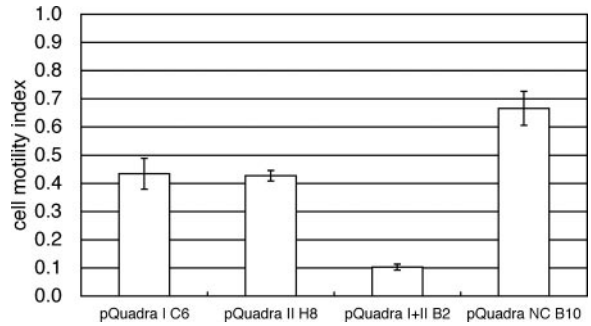


FIG. 6. **Cell motility assay of 14-3-3 knockdown PCF cells.** The assay was carried out in each PCF clone on day 5 after Tet induction. The names of the clones are listed as indicated. The cell motility index (the optical density ratios of before/after mixing the culture medium) was calculated and expressed as mean ± S.D.

14-3-3 in PCF and BSF cells, rats were immunized with purified GST-I and GST-II proteins (Fig. 2*A*). Western blot using purified maltose-binding fusion proteins (MAL) of I, II, and human 14-3-3 $\tau$ showed specificity of the Abs (Fig. 2*B*). We then checked the specificity of these Abs by Western blot using the lysates of PCF cells, showing that both antibodies recognized a band with a relative molecular mass of 30 kDa with little background (Fig. 2*C*). Northern blot analysis of PCF cells detected the ~2.2-kb transcript of I and the ~3.8-kb transcript of II (Fig. 2*D*). The amount of transcript of II appears to be ~3-fold that of I, based on the finding that intensity of the hybridized marker RNA in both blots was equal. Two cDNAs in pGEM-T Easy vector were amplified using M13 forward and reverse primers, and the resultant fragments were used as probes, and the labeling efficiencies of both probes appeared to be identical (Fig. 2*D*). Quantitative Western blot analysis showed that the amount of I was slightly higher than that of II in PCF cells (I, 107 ng/1 $\times$ $10^6$ cells; II, 70 ng/1 $\times$ $10^6$ cells), whereas the amount of I was almost equal to that of II in BSF

[2] M. Inoue, unpublished data.

cells (I, 92 ng/1 × $10^6$ cells; II, 84 ng/1 × $10^6$ cells). Theoretically, an approximately equivalent amount (1–2 × $10^6$ molecules/cell) of each 14-3-3 isoform was expressed (Fig. 2*E*). Combined Northern and Western blot data indicated that the levels of 14-3-3 were post-transcriptionally regulated, as are many proteins of trypanosomes. Immunostaining of PCF cells using anti-I and II Ab clearly showed that both isoforms were localized mainly in cytoplasm (Fig. 3) in the same way as other 14-3-3 isoforms from different species.

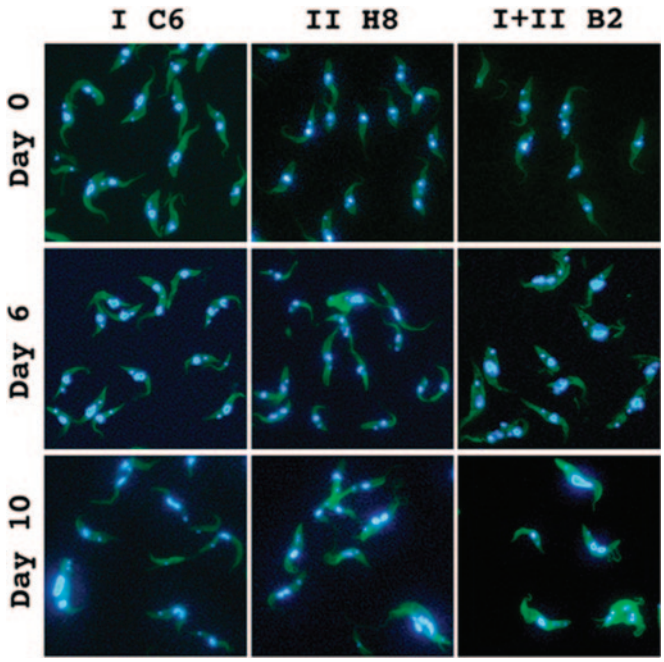


FIG. 7. **Fluorescence pictures of 14-3-3 knockdown PCF cells.** Shown are fluorescence images at 0, 6, and 10 days after Tet induction (1 μg/ml) as indicated. Nuclear and kinetoplast DNA was stained with 4′,6′-diamidine-2-phenylindole dihydrochloride, and α-tubulin was stained with fluorescein isothiocyanate-conjugated DM1 A. Magnification was ×400.

### *Novel Tet-inducible dsRNA Expression System*

*Establishment of PCF Clones*—We constructed a novel tetracycline (Tet)-inducible dsRNA expression vector system, called pQuadra, that facilitates quick and efficient subcloning of inverted repeat sequences, along with a stuffer fragment, in few steps. Several phleomycin-resistant clones transfected with pQuadra I, II, and I + II plus pZJM (25) constructs were selected, and the viable cell counts were compared on day 6, with or without Tet induction. The data are summarized in Supplementary Table 1*A*, showing that pQuadra system is as efficient as pZJM. Some of these Tet-responsive clones were tested for the reduction of I and II protein levels on day 8 of Tet induction, showing that specific reduction of I and II protein levels was obtained in all clones (Supplementary Fig. 2).

*Establishment of BSF Cells*—To increase the transfection efficiency, SV40 sequence (47 bp) (20) was introduced at the EcoRI site in pQuadra (pQuadra SV40) and used for further studies. We isolated several clones and compared the cell counts on day 2, with or without Tet induction. The data are summarized in Supplementary Table 1B. We confirmed the reduction of 14-3-3 protein levels in these clones by Western blot (data not shown).

### *14-3-3 Knockdown of PCF Cells*

*Biochemical Characterization*—We selected four clones and used them in further studies; B10, C6, H8, and B2 are representative of pQuadra NC- and pQuadra I-, II-, and I + II-transfected clones, respectively. dsRNAi of 14-3-3 gene expres-

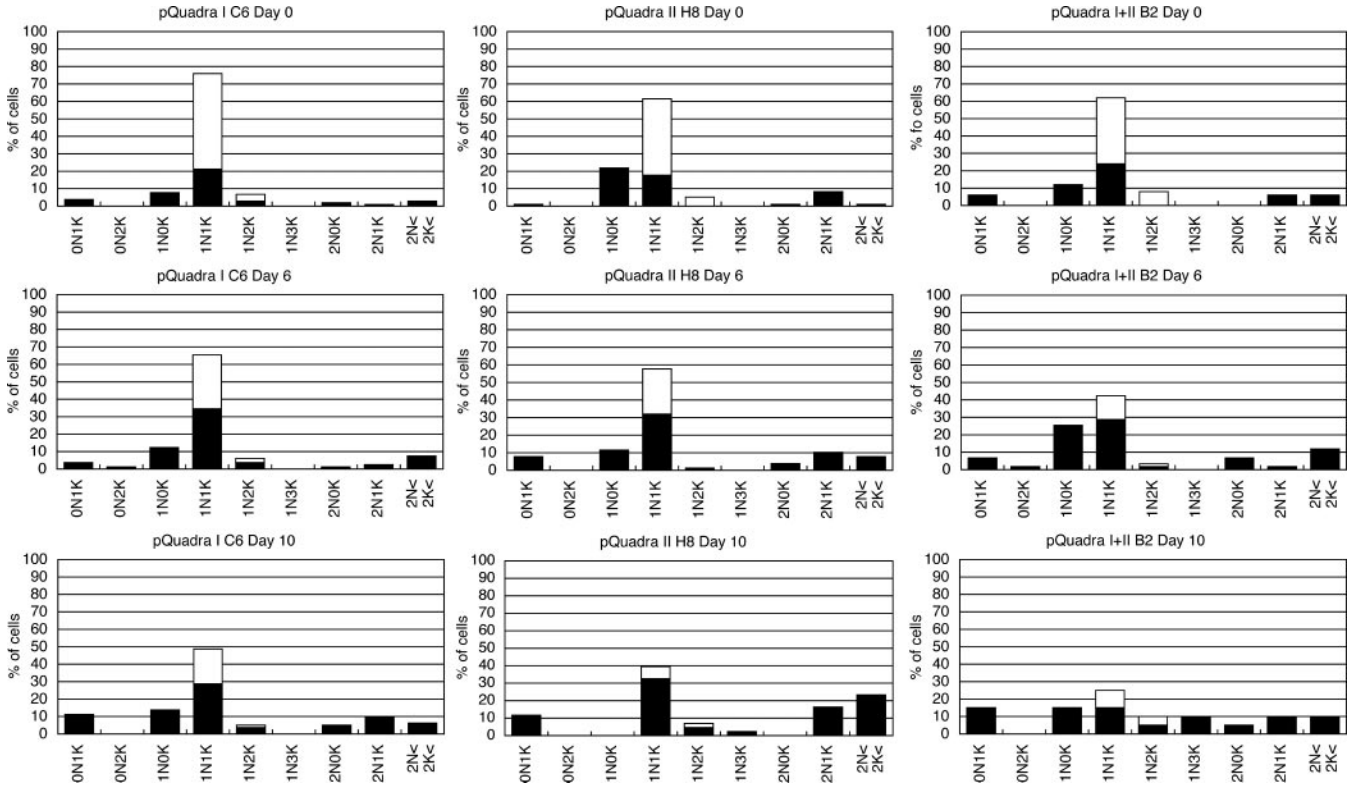


FIG. 8. **Distribution of different cell morphologies: Nuclear and kinetoplast DNA in 14-3-3 knockdown PCF cells.** Nuclear and kinetoplast DNA was counted in 100 cells using the fluorescence images obtained in Fig. 6. The *x* axis and *y* axis represent the amount of nuclear (*N*) and kinetoplast (*K*) DNA and the fraction of cells as a percentage, respectively. The *open* and *closed bars* represent the percentage of normal and abnormal cells, respectively, judged by the size and the shape of cell, the nucleus, and flagella.

sion in PCF cells decreased the growth rates very slowly as shown in Fig. 4. The reduction in growth rate after Tet induction became prominent on day 6 of Tet induction in the order of B2 (I + II knockdown), H8 (II knockdown), and C6 (I knockdown) cells, whereas there was no reduction in B10 (control) cells (Fig. 4). The levels of I mRNA in C6 (I knockdown) and B2 (I + II knockdown) cells became undetectable within 24 h of Tet induction, whereas the levels of I mRNA in B10 (control) and H8 (II knockdown) cells were stable (Fig. 5*A*). The levels of II mRNA in H8 (II knockdown) and B2 (I + II knockdown) cells became undetectable within 24 h of Tet induction, whereas the levels of II mRNA in B10 (control) and C6 (I knockdown) cells were stable (Fig. 5*A*). The overall Northern blot data indicated that specific and quick reduction of mRNA occurred in response to dsRNAi. In C6 (I knockdown) cells, the amount of I protein gradually decreased and was almost undetectable within 4 days after Tet induction, whereas the amount of II was stable (Fig. 5*B*). In H8 (II knockdown) cells, the amount of II protein gradually decreased and was undetectable by 3 days after induction, whereas the amount of I was stable (Fig. 5*B*). In B2 (I + II knockdown) cells, the amounts of I and II proteins gradually decreased and were almost undetectable within 5 and 4 days, respectively (Fig. 5*B*). The combined Northern and Western blot data indicated that the half-life of I was apparently longer, or the translation efficiency of I was better than II in PCF cells.

*Cell Motility Assay*—In order to measure cell motility, we measured the turbidity of the culture medium. when cell motility is good, turbidity of the cell culture medium stays relatively constant in the cuvette at 27 °C for 8 h, whereas if motility is decreased, turbidity of the culture medium is decreased, as the cells sink to the bottom of the cuvette. On day 5, the cell motility index (see "Materials and Methods") was greatly reduced (~0.1) in B2 (I + II knockdown) cells, and it was mildly reduced (~0.4) in both C6 (I knockdown) and H8 (II knockdown) cells, suggesting that 14-3-3 I and/or II affect the cell motility (Fig. 6).

*Morphological Characterization*—Reduction of 14-3-3 levels resulted in abnormalities in size and shape of the cell, nucleus, kinetoplast, and flagella, as shown in Fig. 7. On day 6 after Tet induction, ~50% of normally shaped C6 (I knockdown) cells (Fig. 7) with one nucleus and one kinetoplast (1N1K), exhibited a large bulged nucleus with increased staining intensity compared with C6 (I), H8 (II), and B2 (I + II) on day 0 as well as H8 (II knockdown) on day 6 (Fig. 7). The staining pattern of the large bulged nucleus in C6 (I knockdown) cells appeared to be due to nuclear chromatin condensation. On the contrary, the size of the nucleus in H8 (II knockdown) cells on day 6 was not increased except in one cell (see Fig. 7) in comparison with those on day 0, whereas in B2 (I + II knockdown) cells, the size of the nucleus was markedly increased (Fig. 7). When examining the shape of the 14-3-3 knockdown cells, ~80% of the C6 (I knockdown) cells were normal, whereas ~80% of the H8 (II knockdown) cells were abnormal on day 6 (Fig. 7). The abnormal shape of the H8 (II knockdown) cells appeared to be due to incomplete cell division. These data suggest that 14-3-3 I knockdown cells are likely to fail to start mitosis, whereas 14-3-3 II knockdown cells are likely to fail to complete cell division.

On day 10, 11% of C6 and 15% of H8 and B2 cells were zoid forms; 15% of C6, 17% of H8, and 15% of B2 cells were 2N1K or 2N0K; and 6% of C6, 23% of H8, and 10% of B2 cells were multinucleated giant cells with multikinetoplast (2N<, 2K<) (Fig. 8). That a large percentage of H8 (II knockdown) cells were multinucleated giant cells also suggests that 14-3-3 II knockdown cells are defective in cell division but not mitosis.

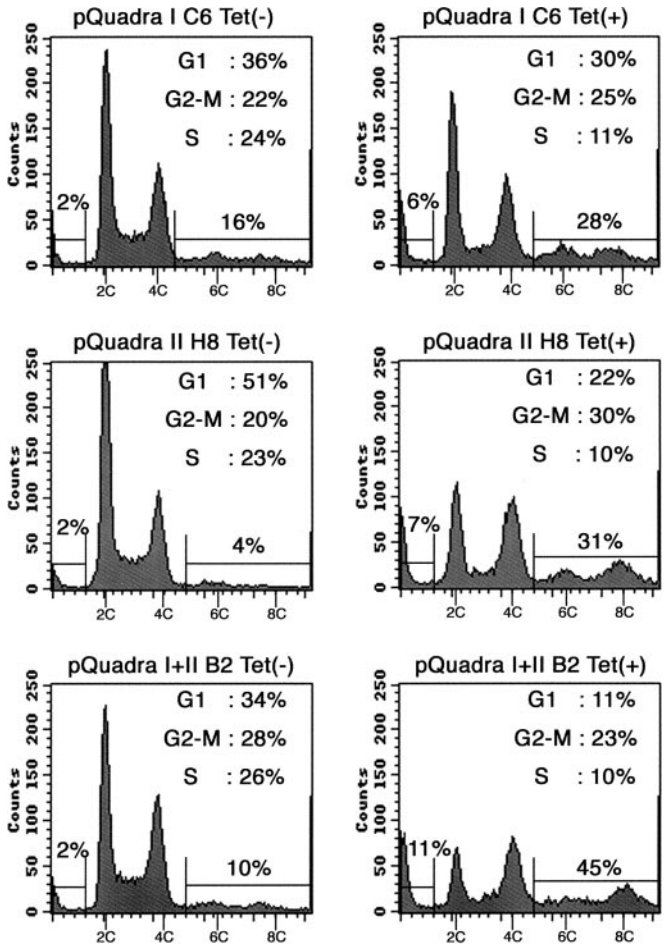


FIG. 9. **Cell cycle analysis of 14-3-3 knockdown cells.** FACS analysis was performed on C6 (I knockdown), H8 (II knockdown), and B2 (I + II knockdown) cells without induction (*Tet* (−)) and/or on day 7 postinduction of Tet (*Tet* (+)). The *x* axis represents fluorescence intensity of DNA, and *y* axis represents the number of cells. 20,000 cells were sorted. The percentages of cells in $G_1$, S, and $G_2$-M phases of the diploid cell cycle are shown. Percentages of cells with DNA content (2C> and 2C<) are shown using the *left* and *right marginal bars*, respectively.

On day 0, 3% of C6, 1% of H8, and 7% of B2 cells were zoids (0N1K), whereas 3% of C6, 10% of H8, and 7% of B2 were 2N1K or 2N0K (Fig. 8). Cells comprising these numbers of nuclei and kinetoplasts are never present in a normal cell cycle, since in normal culture, the kinetoplast divides before the nucleus, suggesting that in some cells the promoter was active and the dsRNAi was made in the absence of Tet (Fig. 8).

A check of the configuration of the flagella showed abnormalities in ~10% of C6, ~30% of H8, and ~50% of B2 cells on day 6, and these abnormalities including bifurcation and detachment (flagella configurations in some cells are barely detectable in Fig. 7; however, we confirmed these abnormalities in magnified pictures with stronger fluorescein isothiocyanate signals (pictures are available upon request)). On day 10 of Tet induction, ~20% of C6, ~90% of H8, and ~75% of B2 cells showed abnormalities in flagella. Cell motility largely depends on the coordinated cytoskeleton-microtubule network as represented by flagella. The fact that 14-3-3 knockdown induced abnormalities of flagella is consistent with the results of the cell motility assay. In conclusion, these results suggest that 14-3-3 I and II play important roles in mitosis and cell division, respectively, perhaps by regulating the cytoskeleton-microtubule network.

### *Cell Cycle Analysis of 14-3-3 Knockdown PCF Cells*

We stained cells with propidium iodide and performed FACS analysis to separate them by their DNA content. Histograms

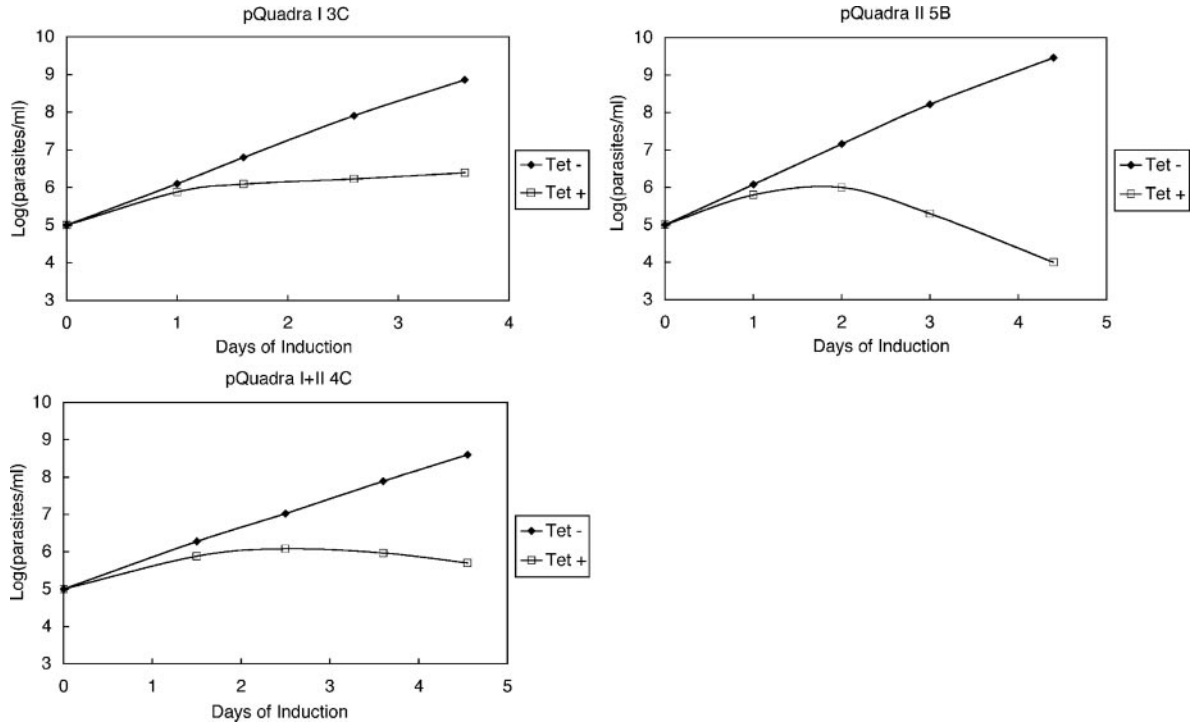


FIG. 10. **Growth curves of representative 90-13 (BSF) cell clones.** Cells were cultured in the presence (1 $\mu$g/ml) or absence of Tet. Cells in the absence of Tet were fed with 1:10 dilution fresh medium everyday, and cells in the presence of Tet were fed with 1:10 dilution fresh medium on day 1 and 1:1 dilution on day 2.

obtained by Cell Quest showed that Tet-induced cells contained overlay of two major cell cycles, the first (diploid cell cycle) that went from 2C ($G_1$) to 4C ($G_2$/M) and the second (tetraploid cell cycle) that went from 4C (second $G_1$) to 8C (second $G_2$/M), where C represents chromosomal number (Fig. 9). In addition, there were two other peaks, one at the first small peak (perhaps zoid or cell debris) and the other at 6C, both of which were generated by abnormal DNA segregation (Fig. 9). We analyzed this unusual cell cycle by Cell Quest followed by ModFIT; first, we divided three populations as shown in the histogram by Cell Quest, and diploid populations were analyzed by ModFIT. In C6 (I knockdown) cells, the population of S-phase cells was drastically reduced by 13%, but the populations of $G_1$ and $G_2$-M phase cells were not significantly changed (Fig. 9). Populations 8C and 6C (tetraploid cell cycle and aberrant cell division; 8C cells are divided into 2C and 6C) were increased by 13% (Fig. 9). These data suggest that transition from M to $G_1$ phase in the diploid cell cycle was not drastically inhibited by knocking down 14-3-3 I expression. On the contrary, in H8 (II knockdown) cells, the population of $G_1$ phase cells was reduced by 19%, the population of S phase cells was reduced by 8%, and the population of the $G_2$-M phase cells was increased by 27% (Fig. 9). These data indicate significant inhibition of M to $G_1$ phase transition and that some of the population that completed M phase but did not undergo cell division appeared to enter the second cell cycle, 14-3-3 II expression was knocked down. In B2 (I + II knockdown) cells, the population of $G_1$ cells was reduced by 13%, and the population of S-phase cells was reduced by 7%, whereas that of $G_2$-M phase cells was increased by 20% (Fig. 9). In addition, populations 8C and 6C were increased by 35% and reached 45% of the total cell population (Fig. 9). These findings suggest that knockdown of both 14-3-3 I and II completely abrogated the normal diploid cell cycle. Forward and side scatter of C6 (I knockdown) cells showed that the sizes and internal complexities of cells were not drastically changed (data not shown), consistent with the notion that knockdown of 14-3-3 I expression did not produce cells with increased size or an increased number of nuclei. Forward and side scatter of the H8 (II knockdown) and B2 (I + II knockdown) cells showed an increased number of cells with increased size and internal complexity (data not shown), indicating that knockdown of 14-3-3 I or II or both produced larger cells with an increased number of nuclei. The overall FACS data suggest that 14-3-3 I and II may play important roles in mitosis and cell division, respectively, which is consistent with the morphological data. We also measured cell cycle on Day 3 of Tet induction (Supplementary Fig. 3); however, changes in histograms were not so drastic as those on day 7, suggesting that subnormal levels of 14-3-3 I and II proteins (Fig. 5) to control cell cycle were still left on day 3.

### *14-3-3 Knockdown of BSF Cells*

We selected three clones and used them for further studies; clone 3C, 5B, and 4C are representative of pQuadra I-, II-, and I + II-transfected clones, respectively. The growth rates of all clones markedly decreased in the order of 5B, 3C, and 4C, beginning from 2 days after Tet induction (Fig. 10). The mRNA levels of 14-3-3 I in 3C and 4C became undetectable within 24 h of Tet induction, whereas the mRNA levels of 14-3-3 I in 5B were stable (Fig. 11*A*). The mRNA levels of 14-3-3 II in 5B and 4C became undetectable within 24 h of Tet induction, whereas those of 14-3-3 II in 3C were stable (Fig. 11*A*). The mRNA levels of 14-3-3 I without Tet induction in 3C were less than those in 5B and 4C, possibly due to promoter leak (Fig. 11*A*). Overall, the Northern blot data indicated that specific and quick reduction of mRNA was mediated by dsRNAi, which is identical to those of PCF clones. In 3C, the amounts of I and II proteins decreased very rapidly to less than half of that in the noninduced condition (Fig. 11*B*). In 5B, the amount of I protein decreased rapidly to less than one-tenth of that in the noninduced condition, and the amount of II protein became undetectable (Fig. 11*B*). In 4C, the amounts of I and II proteins decreased rapidly and become almost undetectable (Fig. 11*B*).

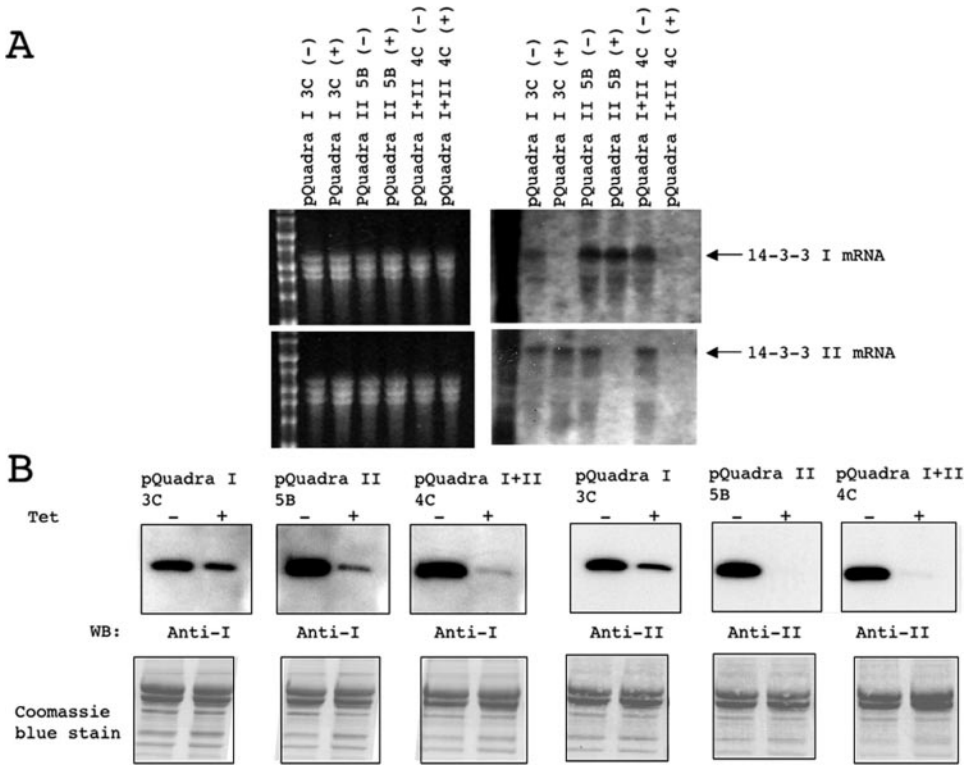


FIG. 11. **Northern and Western blot analysis of 14-3-3 knockdown BSF cells.** *A*, specific reduction of levels of 14-3-3 mRNA of BSF clones after Tet induction on Day 1. *Right*, Northern blot of 14-3-3 I (*top*) and II (*bottom*) in each clone. *Left*, ethidium bromide stain of the gel. Five $\mu$g of total RNA were applied in each lane. *B*, reduction of levels of 14-3-3 proteins on day 2 of Tet induction. *Top*, Western blot analysis of BSF clones using the indicated Ab. *Bottom*, Coomassie Blue stain of the PVDF membrane. The amount of protein applied in each lane was equivalent to the level of lysates of $1 \times 10^6$ cells (6.6 $\mu$g).

In comparison with PCF clones, reduction of protein levels in BSF was more rapid. To our surprise, when the expression of either 14-3-3 isoform was specifically knocked down in BSF cells, the amounts of both proteins simultaneously decreased; this was not observed in 14-3-3 knockdown of PCF cells. The combined Northern and Western blot data suggest that these unusual reductions of protein levels in the knockdown experiments in BSF cells were due to some post-transcriptional regulation but not due to a general shutdown in protein synthesis as shown by tubulin controls (Fig. 14*B*). We confirmed these data using different clones (data not shown). The quick reduction of 14-3-3 protein levels led to morphological changes, which were very similar to those in PCF cells on day 10 but occurred rapidly within 1 day of Tet induction (Fig. 12). Fig. 13 indicates that the abnormalities in the number and size of kinetoplasts, nucleus, and flagella became profound 2 days after Tet induction; ~10% of cells were zoid in each clone, and ~5% of 3C, ~35% of 5B, and ~20% of 4C were multinucleated giant cells. Comparing the morphology of the 14-3-3 I knockdown cells with those of II and/or I + II knockdown, the knockdown of II and/or I + II generated more multinucleated (2N<) cells (Fig. 13), which is consistent with the data obtained from PCF cells on day 10 of Tet induction (Fig. 8). There were also more spherical and enlarged cells than in PCF cells (Figs. 7 and 12).

Each 14-3-3 protein in BSF cells may have a similar distinctive role in cell cycle control to that in PCF cells; however, unwanted simultaneous reduction of protein levels made it difficult to draw definitive conclusions in this study.

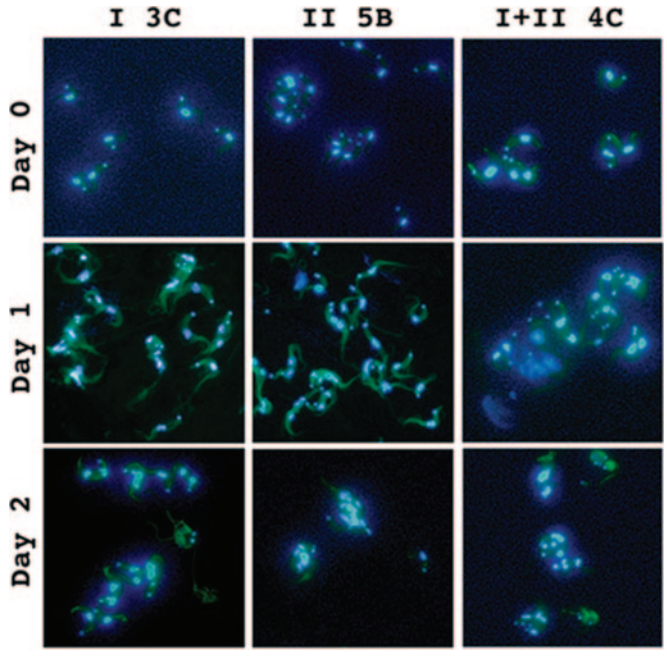


FIG. 12. **Fluorescence pictures of 14-3-3 knockdown BSF cells.** Shown are fluorescence images of 0, 1, and 2 days after Tet induction (1 $\mu$g/ml) as indicated. Nuclear and kinetoplast DNA was stained with 4′,6′-diamidine-2-phenylindole dihydrochloride, and $\alpha$-tubulin was stained with fluorescein isothiocyanate-conjugated DM1 A. Magnification was ×400.

### *Protein Phosphatase and 14-3-3*

When we compared the morphology of 14-3-3 knockdown cells to cells treated with nanomolar levels of okadaic acid (OKA), the phenotypes were similar, but abnormalities were less profound in OKA-treated cells; OKA-treated cells showed multiple nuclei and one or two kinetoplasts (data not shown), confirming the findings of Das *et al.* (10), whereas 14-3-3 knockdown cells contain null or multiple nuclei and kinetoplasts with

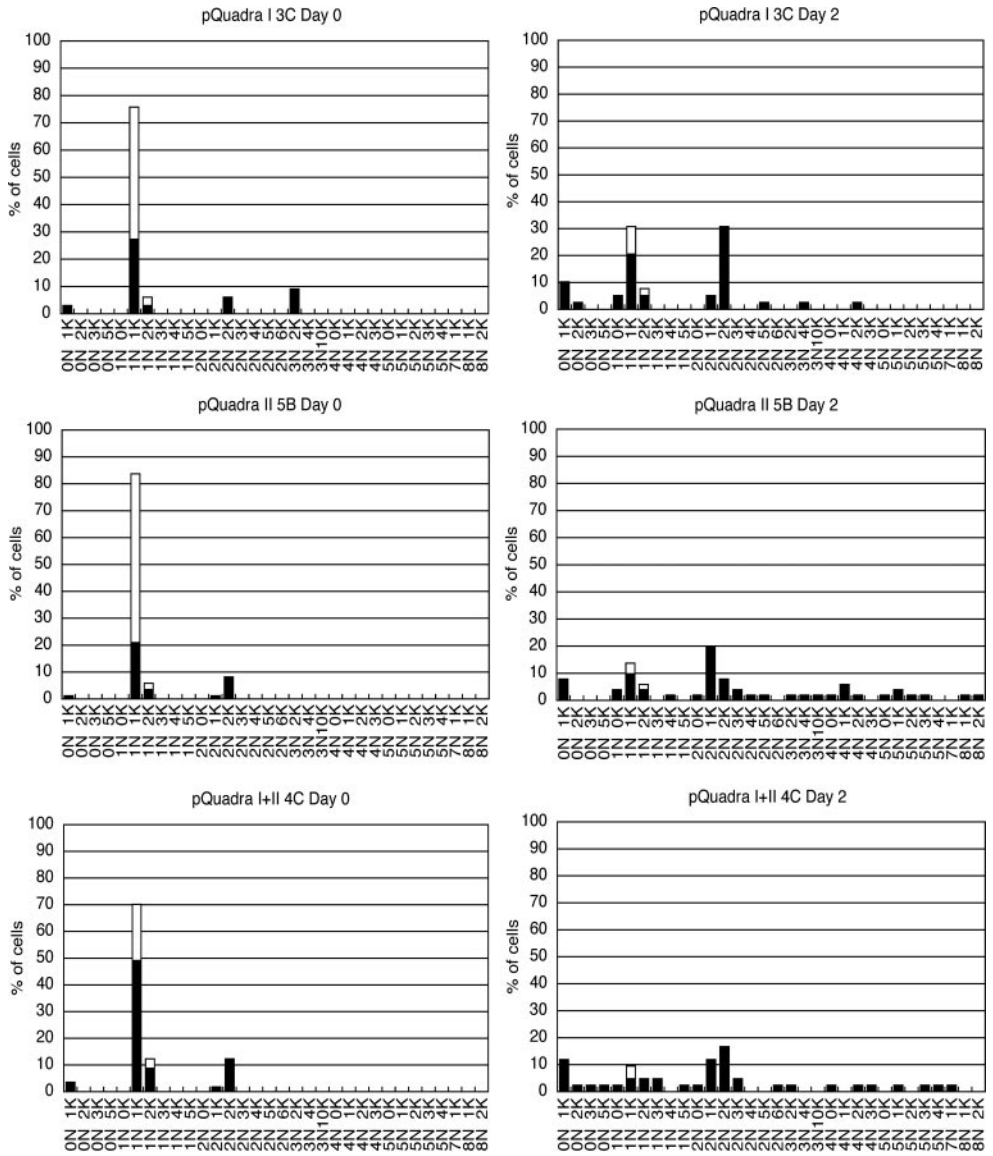


FIG. 13. **Distribution of different cell morphologies: The number of nuclear and kinetoplast DNA in 14-3-3 knockdown BSF cells.** The number of nuclear and kinetoplast DNA was counted in 100 cells using the fluorescence pictures obtained in Fig. 10. The *x* axis and *y* axis represent the number of nuclear (*N*) and kinetoplast (*K*) DNA and the fraction of cells as the percentage, respectively. The *open* and *closed bars* represent the number of normal and abnormal cells, respectively, judged by the size and the shape of cell, the nucleus, and flagella.

abnormal cell shapes plus null or multiple flagella. Another report suggested that levels of β-tubulin but not α-tubulin mRNA were decreased in OKA- or calyculin-treated cells (26). We therefore checked whether 14-3-3 signals may regulate levels of β-tubulin mRNA. Northern blot analysis of 14-3-3 knockdown BSF cells showed that neither α-tubulin nor β-tubulin mRNA levels were changed 18 h after Tet induction (Fig. 14*A*); the morphology of these knockdown cells had changed within 18 h. This finding indicated that 14-3-3 did not regulate levels of β-tubulin mRNA directly. We also confirmed stable levels of α-tubulin and β-tubulin proteins after Tet induction (Fig. 14*B*).

## DISCUSSION

*Simultaneous Reduction of Protein Levels in BSF Cells by Isoform-specific Knockdown of 14-3-3*—When the expression of 14-3-3 genes was knocked down in PCF cells, we observed sequence-specific reduction of 14-3-3 mRNA and protein levels. However, when the expression of either 14-3-3 gene was knocked down in BSF cells, we observed isoform-specific reduction in the respective 14-3-3 mRNA level but reduction in protein levels of both isoforms. This unusual phenomenon in BSF cells could be due to post-translational regulation; we assume that dimerization of 14-3-3 isoforms is required for their stabilization in BSF but not PCF cells, although heterodimers are also formed in PCF cells (data not shown). That the amount of each isoform was almost equal in BSF cells and that the turnover rates of 14-3-3 proteins were higher in BSF cells than in PCF cells support this notion. Interestingly, in *S. cerevisiae* and mammalian cells, 14-3-3 isoforms (ε isoform in the case of mammalians) also preferentially form heterodimers (30). Differences in 14-3-3 isoform monomer stability between PCF and BSF cells may be due to differences in the amounts of and characteristics of proteases and/or their inhibitors that attack these proteins. The α- and β-tubulin protein levels were stable even 2 days after Tet induction in BSF cells (Fig. 14*B*), suggesting that this unusual reduction of protein levels was not due to general translational repression.

*14-3-3 Knockdown of PCF Cells (Morphological Characterization)*—A small percentage of C6 (I knockdown) cells was multinucleated, because some cells expressed enough 14-3-3 I

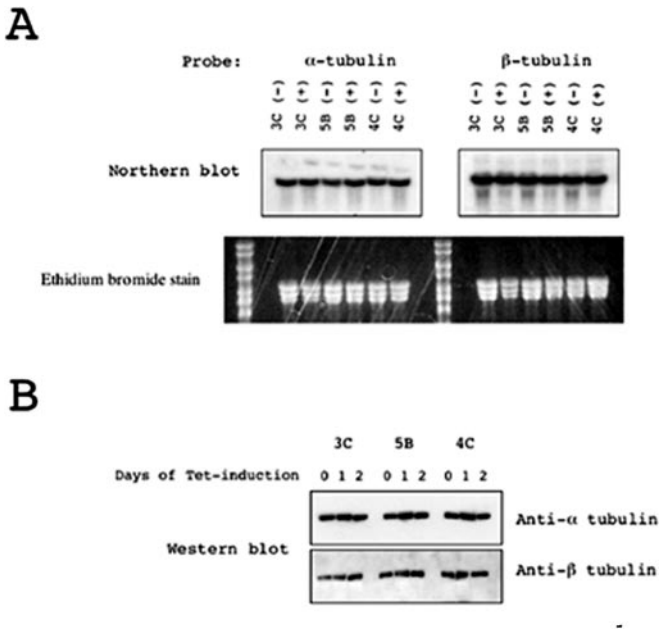


FIG. 14. **Stable α- and β-tubulin mRNA and protein levels of 14-3-3 knockdown BSF cells.** *A*, total RNA was extracted from clones 3C, 5B, and 4C 18 h after Tet induction or untreated. Five μg of RNA were used for Northern blot analysis using α- and β-tubulin cDNA as probes. *B*, lysates of $1 \times 10^6$ cells (6.6 μg) were subjected to Western blot analysis using α- and β-tubulin (DM1 A and Tub 2.1, respectively; Sigma).

to allow them to complete mitosis. Why there were cells with enlarged nuclei in H8 (II knockdown) cells, especially on day 10 (Fig. 7, II H8 on day 10), is unclear; however, we assume that when particular defects have accumulated, other defects are also likely to occur. This may also be why a small percentage of C6 (I knockdown) cells was multinucleated. On day 10, 10–20% of cells were normal in size and/or in shape of the cell, nucleus, and/or flagella in each clone, which is likely to be due to incomplete dsRNAi induction in the cell population.

*Difference in Time Course in 14-3-3 Knockdown between PCF and BSF Cells*—The morphology of PCF cells on day 10 was very similar to that of BSF cells on day 2. PCF cells apparently have much slower replication than BSF cells; it took 3 days to increase the cell number 10-fold in PCF cells, whereas it took just 1 day in BSF cells without Tet induction (Figs. 4 and 10). Therefore, the timing of phenotypic changes coincided with the replication efficiency of the cells. Defects in cell cycle due to lack of 14-3-3 expression appear to accumulate as the cell cycle progresses. In addition, as previously mentioned, protein levels of both isoforms were reduced when expression of either isoform was knocked down in BSF cells, which may explain the more severe defects in BSF cells.

*Difference in Cell Size of Each 14-3-3 Knockdown Clone*—The reason why the sizes of pQuadra I + II-transfected C4 (BSF clone) cells without Tet induction (day 0) are larger than those of 3C (I knockdown BSF clone), and 5B (II knockdown BSF clone) without Tet induction (day 0) is unknown. However, it is possible that a small amount of reduction of both isoforms in BSF cells by means of leak of the Tet-inducible promoter will produce larger cells with gigantic nuclei. Similar large cells containing gigantic nuclei were also seen in H8 (I + II knockdown PCF cells) on day 6 of Tet induction as well as 3C (I knockdown BSF clone) on day 2 of Tet induction. In fission yeast, overexpression of Cdc18 is able to bring about repeated rounds of DNA synthesis in the absence of mitosis and of continuing protein synthesis (31). As a result, enlarged cells with gigantic nuclei can be formed. Therefore, it is possible that 14-3-3 regulates the licensing control of DNA replication in *T. brucei*. This hypothesis is also supported by a report that 14-3-3 in yeast as well as mammals binds to cruciform DNA, which is functionally important for the initiation of DNA replication (32).

*Protein Phosphatase and 14-3-3*—Since no reports of cyclin or cyclin-dependent kinase knockdown in *T. brucei* have mimicked our 14-3-3 knockdown phenotype, we undertook an extensive search of the literature. We found that the 14-3-3 knockdown phenotype of *T. brucei* is similar to that of OKA-treated cells (10). OKA is a potent inhibitor of protein phosphatase 2A and PP1 but preferentially inhibits protein phosphatase 2A over PP1 activities. When OKA treatment was administered to PCF and BSF cells, the kinetoplast but not nuclear DNA segregation was disturbed. As a result, prolonged incubation with OKA creates *T. brucei* with multiple nuclei in gigantic elongated cells, which is similar but distinctive in the defect of kinetoplast segregation (10). On the contrary, in *T. cruzi*, prolonged treatment with calyculin A, a potent inhibitor of *T. cruzi* PP1 at 1–5 nM concentration, produced a similar phenotype: multiple flagella, kinetoplasts, and nuclei in gigantic spherical or elongated cells (11). Such protein phosphatase inhibitors seem to also act as cytokinesis inhibitors in both trypanosomes. In addition, in mammals, isoform-specific PP1 γ antisense-treated A549 lung carcinoma cells showed growth arrest associated with an increase in the number of cells containing 4N DNA (33). Moreover, a recent proteomics study of 14-3-3 binding proteins in mammals reveals that 14-3-3 binds to many important signaling molecules, including cytoskeleton, microtubules, and phosphatases (12); in particular, a recent report suggested that 14-3-3 (ζ) directly binds PP1 γ2, which is a splicing variant of PP1 γ1 (15). These findings prompted us to test whether *T. brucei* 14-3-3 may bind to PP1 γ homologs that have 60% amino acid identity to mammalian PP1 γ1 and regulate the function of PP1 in *T. brucei*. However, both the dsRNAi experiment with the PP1 γ homolog and a GST pull-down study failed to create the phenotype shown here or to show binding (data not shown). We could not directly target 14-3-3 in *T. brucei*; however, it is still possible that a catalytic subunit or regulatory subunit of some serine/threonine phosphatases may bind to 14-3-3, and these direct or indirect associations might change the precise localization of the complexes or alternatively might change the substrate specificity or activity. Alternatively, it is also possible that some kinases, which are regulated by OKA-sensitive phosphatases, may directly or indirectly bind to 14-3-3, and these associations may change the activity, substrate specificity, and/or localization. Such target substrates of 14-3-3-regulated kinases or phosphatases could be microtubule-associated proteins, which control motility, cytoskeletal organization, and cytokinesis (34). Since it was previously reported that OKA and calyculin A treatment of *T. brucei* resulted in reduced β-tubulin mRNA levels, we examined the reduction of β-tubulin mRNA levels induced by knockdown of 14-3-3 gene expression. However, we did not observe any reduction in β-tubulin mRNA or protein levels (Fig. 14*B*), suggesting that 14-3-3 signaling pathways are downstream of OKA-sensitive phosphatase pathways.

*Phenotypes Obtained by Cytokinesis Inhibitors and 14-3-3 Knockdown*—Low concentrations of vinca alkaloids, which inhibit cytokinesis without major effects on cell cycle progression, produce giant cells with multiple nuclei, kinetoplasts, and flagella (35), mimicking our 14-3-3 knockdown phenotype. Taken together with our results, those findings suggest a major role for 14-3-3 in the control of cytokinesis, perhaps by regulating the phosphorylation status of cytoskeletal networks, including microtubule-associated proteins.

The findings reported here provide clues about the functions of 14-3-3 in cell cycle control in trypanosomes such as *T. cruzi*

and *Leishmania*. Furthermore, the present study of the ancient 14-3-3 molecules will be a milestone in revealing the molecular evolution of signal transduction pathways, especially relating to cytokinesis and cell motility. Search for the binding partners of 14-3-3 is now under way, which might reveal the secret to unique cell cycle control in *T. brucei*. This approach also promises to identify important distinctive signaling molecules as drug targets.

*Acknowledgments*—We thank Dr. Paul Englund for pZJM vector and Dr. George Cross for pLew100 vector plus 29-13 and 90-13 cells. We also thank Drs. Yoshitatsu Sei (National Institutes of Health) and Nobuo Horikoshi (Washington University School of Medicine) for critical discussion and review.

REFERENCES

1. Fu, H., Subramanian, R. R., and Masters, S. C. (2000) *Annu. Rev. Pharmacol. Toxicol.* **40,** 617–647
2. Tzivion, G., and Avruch, J. (2002) *J. Biol. Chem.* **277,** 3061–3064
3. Yaffe, M. B. (2002) *FEBS Lett.* **513,** 53–57
4. van Hemert, M. J., Steensma, H. Y., and van Heusden, G. P. H. (2001) *BioEssays* **23,** 936–946
5. Masters, S. C., and Fu, H. (2001) *J. Biol. Chem.* **276,** 45193–45200
6. Bunney, T. D., van Walraven, H. S., and de Boer, A. H. (2001) *Proc. Natl. Acad. Sci. U. S. A.* **98,** 4249–4254
7. Moorhead, G., Douglas, P., Cotelle, V., Harthill, J., Morrice, N., Meek, S., Deiting, U., Stitt, M., Scarabel, M., Aitken, A., and MacKintosh, C. (1999) *Plant J.* **18,** 1–12
8. Roberts, M. R. (2000) *Curr. Opin. Plant Biol.* **3,** 400–405
9. van Hemert, M. J., van Heusden, G. P. H., and Steensma, H. Y. (2001) *Yeast* **18,** 889–895
10. Das, A., Gale, M., Jr., Carter, V., and Parsons, M. (1994) *J. Cell Sci.* **107,** 3477–3483
11. Orr, G. A., Werner, C., Xu, J., Bennett, M., Weiss, L. M., Takvorkan, P., Tanowitz, H. B., and Wittner, M. (2000) *Infect. Immun.* **68,** 1350–1358
12. Rubio, M. P., Geraghty, K. M., Wong, B. H. C., Wood, N. T., Campbell, D. G., Morrice, N., and MacKintosh, C. (2004) *Biochem. J.* **379,** 395–408
13. Sugiyama, K., Sugiura, K., Hara, T., Sugimoto, K., Shima, H., Honda, K., Furukawa, K., Yamashita, S., and Urano, T. (2002) *Oncogene* **21,** 3103–3111
14. Wera, S., Fernandez, A., Lamb, N. J. C., Turowski, P., Hemmings-Mieszczak, M., Mayer-Jaekel, R. E., and Hemmings, B. A. (1995) *J. Biol. Chem.* **270,** 21374–21381
15. Huang, Z., Myers, K., Khatra, B., and Vijayaraghavan, S. (2004) *Biol. Reprod.* **71,** 177–184
16. Woodward, R., and Gull, K. (1990) *J. Cell Sci.* **95,** 49–57
17. Ploubidou, A., Robinson, D. R., Docherty, R. C., Ogbadoyi, E. O., and Gull, K. (1999) *J. Cell Sci.* **112,** 4641–4650
18. Carrington, M. (1993) *Protocols in Molecular Parasitology* (Hide, J. E., eds) pp. 1–13. Humana Press, Totowa, NJ
19. Wirtz, E., Leal, S., Ochatt, C., and Cross, G. A. (1999) *Mol. Biochem. Parasitol.* **99,** 89–101
20. Dean, D. A., Dean, B. S., Muller, S., and Smith, L. C. (1999) *Exp. Cell Res.* **253,** 713–722
21. Schnaufer, A., Panigrahi, A. K., Panicucci, B., Igo, R. P., Jr., Wirtz, E., Salavati, R., and Stuart, K. (2001) *Science* **291,** 2159–2162
22. Xiao, B., Smerdon, S. J., Jones, D. H., Dodson, G. G., Soneji, Y., Aitken, A., and Gamblin, S. J. (1995) *Nature* **376,** 188–191
23. Liu, D., Bienkowska, J., Petosa, C., Collier, R. J., Fu, H., and Liddington, R. (1995) *Nature* **376,** 191–194
24. Rittinger, K., Budman, J., Xu, J., Volinia, S., Cantley, L. C., Smerdon, S. J., Gamblin, S. J., and Yaffe, M. B. (1999) *Mol. Cell.* **4,** 153–166
25. Wang, Z., Morris, J. C., Drew, M. E., and Englund, P. T. (2000) *J. Biol. Chem.* **275,** 40174–40179
26. Li, S., and Donelson, J. E. (1995) *Biochem. Biophys. Res. Commun.* **212,** 793–799
27. Muslin, A. J., Tanner, J. W., Allen, P. M., and Shaw, A. S. (1996) *Cell* **84,** 889–897
28. Obsil, T., Ghirlando, R., Klein, D. C., Ganguly, S., and Dyda, F. (2001) *Cell* **105,** 257–267
29. Brunet, A., Kanai, F., Stehn, J., Xu, J., Sarbassova, D., Frangioni, J. V., Dalal, S. N., DeCaprio, J. A., Greenberg, M. E., and Yaffe, M. B. (2002) *J. Cell Biol.* **156,** 817–828
30. Chaudhri, M., Scarabel, M., and Aitken, A. (2003) *Biochem. Biophys. Res. Commun.* **300,** 679–685
31. Nishitani, H., and Nurse, P. (1995) *Cell* **83,** 397–405
32. Callejio, M., Alvarez, D., Price, G. B., and Zannis-Hadjopoulos, M. (2002) *J. Biol. Chem.* **277,** 38416–38423
33. Cheng, A., Dean, N. M., and Honkanen, R. E. (2000) *J. Biol. Chem.* **275,** 1846–1854
34. Mandelkow, E., and Mandelkow, E.-M. (1995) *Curr. Opin. Cell Biol.* **7,** 72–81
35. Grellier, P., Sinou, V., Garreau-de Loubresse, N., Bylen, E., Boulard, Y., and Schrevel, J. (1999) *Cell Motil. Cytoskeleton* **42,** 36–47

7

Supplementary Fig. 1. **Schematic view of quadric ligation**.

Supplementary Fig. 2. **Reduction of 14-3-3 protein levels in individual PCF clones established by transfection of Tet-inducible 14-3-3 dsRNA expression vectors (pZJM and pQuadra)**. Cells were cultured in the presence (1 μg/ml) (+) or in the absence of Tet (-) for 8 days. Lysates were made from $1x10^6$ cells (or equivalent amount of protein) of individual clones by SDS-gel loading buffer and applied on 10-20 % SDS-gel. Western blot analysis was carried out using the indicated Ab.

Supplementary Table 1. **A**. **Ratios of viable cell counts of 29-13 PCF clones with or without Tet-induction**. Viable cell counts on Day 6 were measured by a Cell-Titer Glo assay kit (Promega) or hematocytometer. **B**. **Ratios of viable cell counts of 90-13 BSF clones with or without Tet-induction**. Viable cell counts on Day 2 were measured with a hematocytometer.

Supplementary Fig. 3. **Cell cycle analysis of 14-3-3 knockdown cells.** FACS analysis

was performed on C6 (I knockdown), H8 (II knockdown) and B2 (I+II knockdown) cells without induction, Tet (-) and/or on Day 3 post-induction of Tet, Tet (+). The X-axis represents fluorescence intensity of DNA and Y-axis represents the number of cells. Twenty thousand cells were sorted.

## A

29-13 pQuadra I

| Clone | Tet +/- |
|---|---|
| B11 | 0.47 |
| C1 | 0.44 |
| C6 | 0.55 |
| C9 | 0.42 |
| E3 | 0.40 |
| E9 | 0.43 |
| E12 | 0.59 |
| F4 | 0.57 |

pQuadra II

| Clone | Tet +/- |
|---|---|
| A4 | 1.0 |
| A8 | 0.31 |
| B5 | 0.24 |
| B9 | 0.29 |
| E2 | 0.24 |
| E6 | 0.67 |
| F11 | 0.25 |
| F12 | 0.24 |
| H4 | 0.29 |
| H8 | 0.20 |

pQuadra I+II

| Clone | Tet +/- |
|---|---|
| B2 | 0.31 |
| E8 | 0.29 |
| G9 | 0.31 |

pQuadra NC

| Clone | Tet +/- |
|---|---|
| A5 | 0.99 |
| B10 | 1.1 |
| C8 | 1.0 |
| D1 | 1.0 |
| F2 | 1.1 |

29-13 pZJM I

| Clone | Tet +/- |
|---|---|
| A6 | 0.55 |
| A11 | 0.89 |
| B8 | 1.0 |
| C6 | 0.35 |
| C10 | 0.39 |
| C12 | 0.64 |
| D2 | 0.64 |
| D3 | 0.58 |
| D10 | 0.48 |
| H12 | 0.49 |

pZJM II

| Clone | Tet +/- |
|---|---|
| A4 | 0.54 |
| C7 | 0.38 |
| C12 | 0.82 |
| D2 | 0.61 |
| D6 | 0.75 |
| E6 | 0.76 |
| F3 | 0.63 |
| G11 | 0.92 |

## B

90-13 pQuadra I

| Clone | Tet +/- |
|---|---|
| 3C | 0.019 |

pQuadra II

| Clone | Tet +/- |
|---|---|
| 1A | 0.069 |
| 4B | 1.0 |
| 5B | 0.069 |
| 2C | 0.29 |
| 6C | 1.0 |
| 1D | 1.0 |

pQuadra I+II

| Clone | Tet +/- |
|---|---|
| 3B | 1.0 |
| 5B | 0.10 |
| 1C | 0.17 |
| 3C | 0.15 |
| 5C | 0.33 |
| 6D | 0.12 |

suppl. Table 1

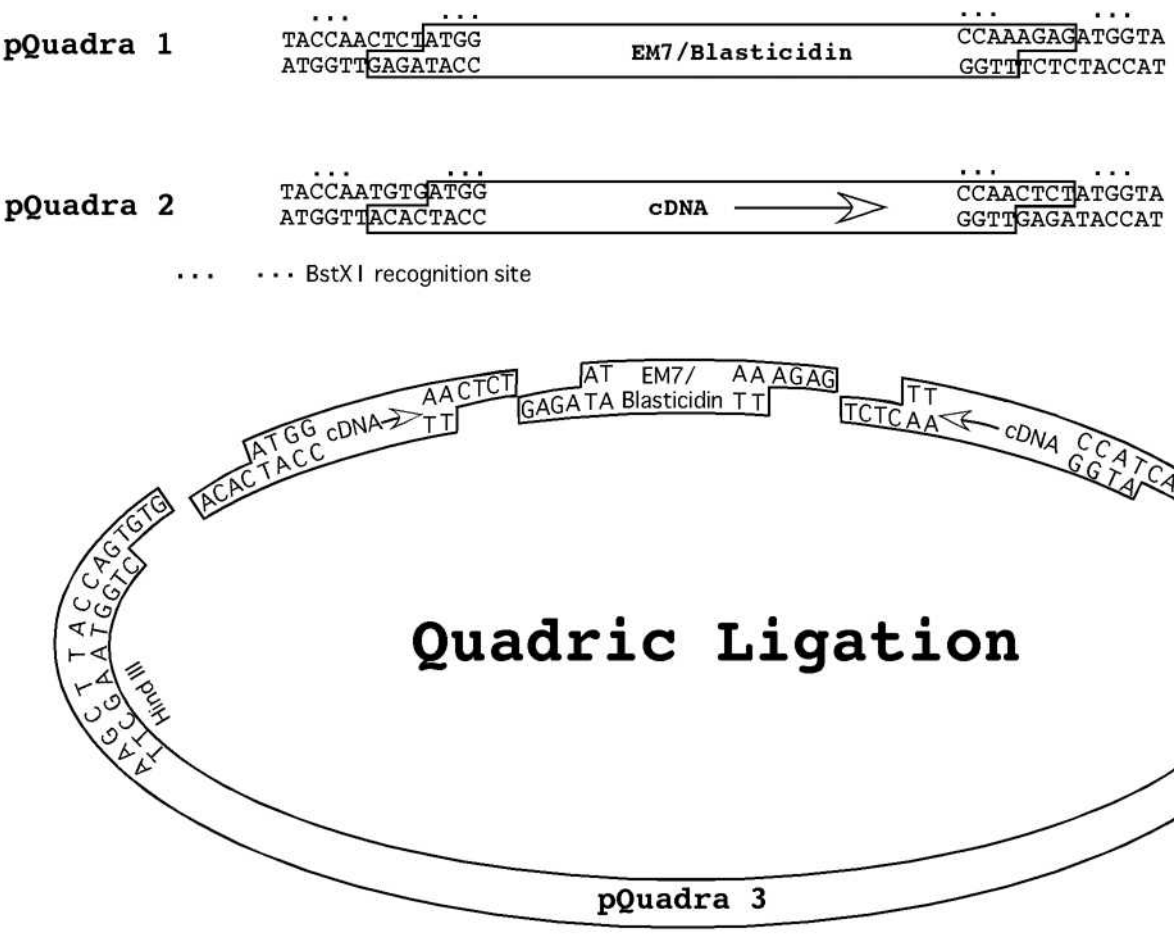


suppl. Fig. 1

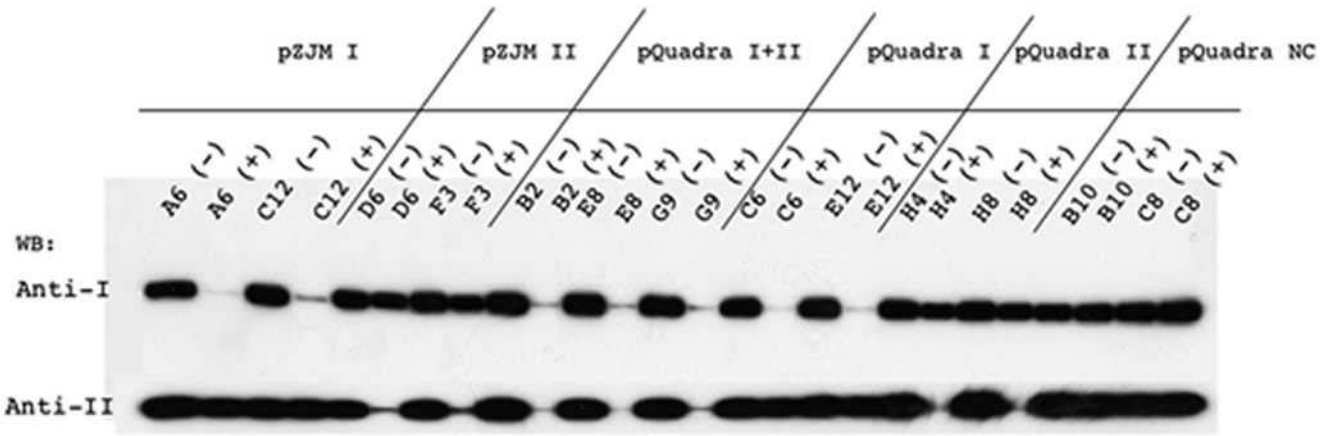


suppl. Fig. 2

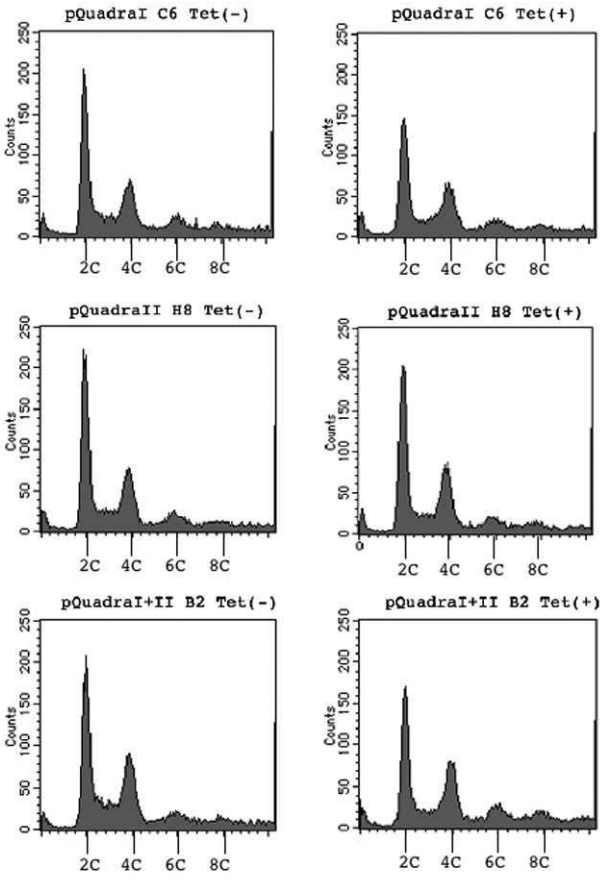


suppl. Fig. 3